Atmospheric Environment 176 (2018) 140–147

Contents lists available at ScienceDirect

Atmospheric Environment

journal homepage: www.elsevier.com/locate/atmosenv

Identification and semi-quantification of biogenic organic nitrates in ambient particulate matters by UHPLC/ESI-MS

Rui Li[a], Xinfeng Wang[a,*], Rongrong Gu[a], Chunying Lu[a], Fanping Zhu[b], Likun Xue[a], Huijun Xie[a], Lin Du[a], Jianmin Chen[a,b], Wenxing Wang[a]

[a] Environment Research Institute, Shandong University, Ji'nan 250100, China
[b] School of Environmental Science and Engineering, Shandong University, Ji'nan 250100, China

ARTICLE INFO

Keywords:
Biogenic organic nitrates
UHPLC/ESI-MS
Identification
Semi-quantification
Fine particulate matters

ABSTRACT

Particulate biogenic organic nitrates (PBONs) are important components of secondary organic aerosols and play an important role in the tropospheric atmosphere chemistry. However, the concentrations and the chemistry of PBONs remain poorly understood due to the lack of accurate measurement techniques on specific organic nitrates. In this study, ultra high performance liquid chromatography/electrospray mass spectrometry was applied in detection of individual PBONs in ambient atmosphere. Total five kinds of PBONs were identified in $PM_{2.5}$ samples collected in urban Ji'nan in spring according to characteristic fragments of NO_2, NO_3, HNO_3, CO_2, and H_2O, including monoterpene hydroxyl nitrate (MW = 215, MHN215), pinene keto nitrate (MW = 229, PKN229), limonene di-keto nitrate (MW = 247, LDKN247), oleic acid keto nitrate (MW = 359, OAKN359), and oleic acid hydroxyl nitrate (MW = 361, OAHN361). Among them, three kinds of PBONs originated from biogenic volatile organic compounds of pinene and limonene and two kinds of PBONs came from chemical conversion of oleic acid. The concentrations of these PBONs were roughly quantified with surrogate standards of (1R,2R,5R)-(+)-2-hydroxy-3-pinanone and ricinoleic acid. The average concentrations of MHN215, PKN229, LDKN247, OAKN359, and OAHN361 were 111.6 ± 23.0, 93.1 ± 49.6, 55.3 ± 7.4, 23.4 ± 14.5, 36.8 ± 18.3 ng m^{-3}, respectively. The total concentration of these PBONs was 325.4 ± 116.7 ng m^{-3}, contributing to 1.64 ± 0.34‰ of $PM_{2.5}$.

1. Introduction

Particulate organic nitrates have significant impacts on organic aerosols, regional nitrogen recycling, and cloud condensation nuclei (CCN) activation. They contribute a large fraction to organic aerosols which have adverse influence on air quality, visibility, and human health (Ayres et al., 2015; Bellouin et al., 2011; Mauderly and Chow, 2008; Ng et al., 2017). Fry et al. (2013) observed above 20 pptv (equal to 179 ng m^{-3}, assuming average MW = 200; the same hereinafter) particulate phase peroxy and alkyl nitrates in Pike National Forest, Colorado, a site with large biogenic volatile organic compounds (BVOCs) emissions. Mylonas et al. (1991) found that organic nitrates contributed approximately 12% to carbon in aerosols in an urban site. Day et al. (2010) also observed a contribution of maximum 9% to submicro organic matters in a coastal region. In addition, transport, dry deposition and hydrolysis of organic nitrates lead to loss of NO_x and thus affect the nitrogen recycling (Fisher et al., 2016). Organic nitrates could also serve as temporary NO_x reservoir due to their longer lifetime. They transport to remote regions from original pollution area and then decompose to release NO_x back to atmosphere (Atherton, 1989; Horowitz et al., 2007; Treves et al., 2000; Xiong et al., 2015). In addition, due to the hygroscopicity of nitrooxy group and other groups like hydroxyl and carbonyl groups, organic nitrates can absorb water on the surface and act as important CCN, which thereby promotes the cloud formation and influences the regional climate (Charlson and Schwartz, 1992; Hallquist et al., 1999; Novakov and Penner, 1993; Renbaum and Smith, 2009; Twomey et al., 1984). Particulate biogenic organic nitrates (PBONs) are among the major constituents of organic nitrates in aerosols due to the very large emissions of biogenic volatile organic compounds in global scale (Ayres et al., 2015; Pye et al., 2015).

A number of techniques have been applied to determine the concentration of organic nitrates in the past decades, which has been well summarized in the review by Ng et al. (2017). The relevant studies mainly focused on the total concentration measurement in field campaigns and the individual organic nitrate detection in chamber simulations. Field measurements of total concentration of organic nitrates

* Corresponding author.
E-mail address: xinfengwang@sdu.edu.cn (X. Wang).

https://doi.org/10.1016/j.atmosenv.2017.12.038
Received 14 July 2017; Received in revised form 20 November 2017; Accepted 23 December 2017
Available online 27 December 2017
1352-2310/ © 2017 Elsevier Ltd. All rights reserved.

were conducted with Fourier transform infrared spectrometer (FTIR), thermo dissociation followed by laser induced fluorescence (TD-LIF) or chemiluminescence, and aerosol mass spectrometry (AMS) based on the detection of nitrooxy group (Nielsen et al., 1995, 1998; O'Brien et al., 1995; Thieser et al., 2016; Wooldridge et al., 2010; Xu et al., 2015). Day et al. (2010) deployed FTIR to analyze the total content of nitrooxy group in sub-micro particles in coastal southern California with the average concentration of 60 ng m^{-3} (equal to 194 ng m^{-3} organic nitrates). TD-LIF was used by Beaver et al. (2012) to measure the total alkyl nitrates in real-time in Sierra Nevada with the concentration above 200 pptv (equal to 1786 ng m^{-3}). AMS was deployed by Fry et al. (2013) to determine the concentration of particulate phase nitrooxy group during BEACHON-RoMBAS in 2011 with the average value of ~100 ng m^{-3} (equal to 320 ng m^{-3} organic nitrates). In laboratory chamber studies, gas or liquid chromatography (GC or LC) followed by mass spectrometry (MS) or new developed chemical ionization mass spectrometry (CIMS) were widely used for identification and quantification of specific organic nitrates (Docherty and Ziemann, 2006; Kwan et al., 2012; Surratt et al., 2006). Mills et al. (2016) identified five kinds of isoprene hydroxyl nitrates in laboratory synthetic standard mixture by GC-MS. Kwan et al. (2012) identified 13 kinds of isoprene nitrates by CIMS and quantified their concentrations through empirical method based on dipole moment and polarizability of molecules. Docherty and Ziemann (2006) identified two kinds of oleic acid nitrates by HPLC-MS from the oxidation products of oleic acid by NO_3. Compared to LC-MS, GC-MS/CIMS was suitable for detection of volatile and thermo-stable compounds and was possibly problematic for most organic nitrates due to the thermo instability and decomposition in separation system (Zhao and Yinon, 2002). So far, however, due to the complex matrices of ambient atmosphere and the lack of authentic standards, it is subjected from great difficulty to achieve accurate measurement of organic nitrates in particulate matters. There is an urgent need to establish a reliable analysis method to identify the specific organic nitrates and further quantify the contents.

In this study, ultra high performance liquid chromatography/electrospray mass spectrometry (UHPLC/ESI-MS) was applied and optimized to detect individual PBONs in fine particulate matters ($PM_{2.5}$) collected from urban atmosphere. Total five kinds of PBONs were identified by multi-stage MS (MS^n) after separation. Surrogate standards of (1R,2R,5R)-(+)-2-hydroxy-3-pinanone and ricinoleic acid were chosen to approximately quantify the concentrations of these PBONs.

2. Experiment and methods

2.1. Reagents and solutions

HPLC-grade methanol (≥99.9%), HPLC-grade formic acid (≥98.0%), and ricinoleic acid (≥99%) were purchased from Sigma-Aldrich (USA). Amyl nitrate (> 98.0%, GC) and (1R,2R,5R)-(+)-2-hydroxy-3-pinanone (> 98.0%, GC) were ordered from TCI (Japan). Isoamyl nitrate (> 98%) and tropinone (> 98%) were ordered from CNW (Germany) and IL (USA), respectively. Carveol (> 97%) and Isosorbide 5-mononitrate (> 98%) were purchased from Aladdin (China) and Energy Chemical (China), respectively. Water purified with Millipore Simplicity Water Purification System was used throughout this study.

2.2. Sample collection

$PM_{2.5}$ samples were collected at the Atmospheric Environment Observation Station (36°40′ N, 117°03′ E) on the rooftop of a teaching building in the Center Campus of Shandong University in April, 2016. The sampling site was located in almost the urban center of Ji'nan, a typical industrial city in North China. A middle-volume $PM_{2.5}$ sampler (TH-150 A, China) was deployed to collect fine particulate matters on quartz fiber filters with diameter of 88 mm at a flow rate of 100 L min^{-1}. The $PM_{2.5}$ filter samples were collected twice per day with a sampling duration of 11.5 h and a sampling volume of 69 m^3. The daytime samples were collected from 8:00 a.m. to 7:30 p.m. and the nighttime samples were collected from 8:00 p.m. to 7:30 a.m. in the next morning.

2.3. Sample preparation

The sample filter was cut into two halves. One half of the filter sample was extracted by sonication with 15 mL methanol for 15 min and repeated it for three times. Then, the extract solution was stored at 4 °C for 12 h and the upper extract solution was concentrated to near dry by rotary evaporation. The dried residue was re-dissolved with 1.5 mL methanol and then filtered by 0.45 μm pore-size PTFE syringe filters. The filtrate was blown to near dry by a gentle high purity nitrogen stream (without heat) and then was reconstituted with 400 μL 2 mg L^{-1} tropinone methanol solution. Tropinone was used as the inner standard to minimize instrumental errors. The final sample solution was stored at −20 °C for subsequent chemical analysis. Note that the ultrasonic extraction with methanol could produce a small amount of OH and methyl radicals (Miljevic et al., 2014; Riesz et al., 1985). To examine the potential influence of sonication on the measurements of PBONs, some filter samples were simultaneously extracted by both ultrasonic agitation and orbital shaker. The results obtained from sonication and vibration were almost the same for some PBONs, while there was a difference for some others with a factor between 0.5 and 1.8, indicating small influence from sonication. In this study, the presented concentrations of PBONs were from sample solutions extracted by sonication.

2.4. Instrumentation

2.4.1. UHPLC condition

The Thermo Scientific LCQ Fleet UHPLC-MS system was used for organic nitrates detection. The UHPLC coupled with an Atlantis C18 column (2.1 × 150 mm, 2.1 μm) was used for PBONs separation. The eluent consisted of methanol (A) and 0.1% (by volume) aqueous formic acid (B) was operated at a flow rate of 0.2 mL min^{-1}. Sample solution with volume of 5 μL was injected with gradient methanol/0.1% aqueous formic acid. The elution program was set as below: 30% A, 70% B, hold for 3 min; A increased to 90%, B decreased to 10% in 10 min, hold for 3 min; and then A quickly decreased to 30%, B quickly increased to 70% in 0.1 min, hold for 3.9 min. The column temperature was set as 24 °C in which condition major PBONs can be completely separated within 20 min.

2.4.2. MS condition

The ion trap mass spectrometer equipped with an electrospray ionization (ESI) source was used to obtain detail structure information of individual organic nitrates. The ESI condition was optimized as below: capillary temperature of 320 °C, capillary voltage of 4 kV, sheath gas flow rate of 30 arb min^{-1}, and auxiliary gas flow rate of 10 arb min^{-1}. Sample extracts were analyzed in full scan mode with mass (m/z) range from 50 to 500. Selected ion monitoring mode (SIM) was also tried, but the intensity was slightly lower than that from full scan mode in our ion trap mass. Positive and negative ion modes were both operated and only the data of positive ion mode were used because of very weak responses of potential organic nitrates under negative ion mode. Pseudo molecular ions $[M+H]^+$ (m/z = MW + 1) were generated from the protonation of analyte molecules and were detected as parent ions by single MS mode. MS^n (MS^2 and MS^3) was used to further identify the structure of target species. Collision induced dissociation (CID) energy was set as 25 to 35 eV according to the structure stability of analyte molecules. Reasonable identification can be achieved only base on the established fragmentation mechanism when authentic standard is

Table 1
Retention time and possible isomers of the identified PBONs.

Organic nitrates	Retention time (min)	Possible isomers
Monoterpene hydroxyl nitrate (MW = 215, MHN215)	12.18, 12.75	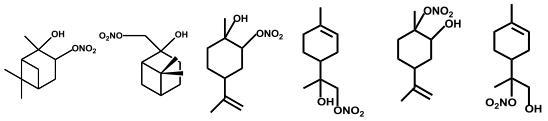
Pinene keto nitrate (MW = 229, PKN229)	13.21	
Limonene di-keto nitrate (MW = 247, LDKN247)	12.10	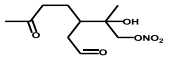
Oleic acid keto nitrate (MW = 359, OAKN359)	15.75	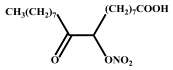
Oleic acid hydroxyl nitrate (MW = 361, OAHN361)	13.73	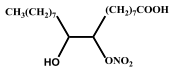

unavailable. The neutral losses of fragments of NO_2 (46 Da) and NO_3 (62 Da) corresponded to the nitrooxy group of PBONs under MS^n collision (Docherty and Ziemann, 2006; Perraud et al., 2010).

3. Results and discussion

3.1. UHPLC separation

The Atlantis C18 column is a reversed phase column that target analytes with higher polarity will elute earlier. Methanol rather than acetonitrile was used as the organic phase of eluents to obtain better peak shape and higher sensitivity. In this study, five kinds of PBONs were separated between 12 min and 16 min, including momoterpene hydroxyl nitrate (MW = 215, MHN215), pinene keto nitrate (MW = 229, PKN229), limonene di-keto nitrate (MW = 247, LDKN247), oleic acid keto nitrate (MW = 359, OAKN359), and oleic acid hydroxyl nitrate (MW = 361, OAHN361). The naming convention followed the names of limonene nitrates reported by Fry et al. (2011) and was further simplified. The retention time (RT) and possible isomers of these five kinds of PBONs were shown in Table 1.

3.2. Identification of PBONs

3.2.1. m/z = 216 ion

Fig. 1 shows the extracted ion chromatogram (EIC) and the MS^n spectrum of the parent ions at m/z = 216. Total three chromatographic peaks were observed at RT = 12.18, 12.75, and 13.45 min. The identification of the specific compounds corresponding to these chromatographic peaks required further information from MS^n.

The m/z = 216 parent ions were fragmented into product ions by MS^2 with CID energy of 25 eV. MS^2 spectrum for the peak at RT = 12.75 min is shown in Fig. 1b. The most intense mass peak at m/z = 170 corresponds to a neutral loss of 46 Da (NO_2) fragment from the parent ion at m/z = 216. According to the APCI-MS detection of 2-hydroxypinane-3-nitrate in a chamber study by Perraud et al. (2010), we assigned the peak at RT = 12.75 min to 2-hydroxypinane-3-nitrate (MHN215 in this study). MS^2 spectrum obtained from the peak at RT = 13.45 min is shown in Fig. 1c. Three major mass peaks at m/z = 198, 181, 163 correspond to neutral losses of 18 Da (H_2O), 35 Da, 53Da (H_2O + 35) fragments, respectively. An obvious 35 Da fragment can be explained as Cl atom or (H_2O + OH), both of which were not the characteristic fragment of MHN215 or other organic nitrates. Therefore, the possibility of the chromatographic peak of MHN215 appearing at 13.45 min is ruled out. MS^2 spectrum for the peak at RT = 12.18 min is shown in Fig. 1d. An intense mass peak at m/z = 198 and a weak mass peak at m/z = 216 were obtained. The fragment ion at m/z = 198 can be explained by neutral loss of H_2O from the parent ion. The sole loss of H_2O fragment suggests that the compound associated with the peak at RT = 12.18 min has a relatively stable structure. To clarify the specific structure, the product ions at m/z = 198 were further fragmented with CID energy of 35 eV (MS^3 of the m/z = 216 ion, see Fig. 1e). Two intensive fragment ions at m/z = 180 and 152 were obtained. The m/z = 152 ion obviously corresponded to a neutral loss of 46 Da (NO_2) fragment from the ion at m/z = 198, while the 18 Da neutral loss resulting in product ion at m/z = 180 could be explained as H_2O. We therefore assigned the peak at RT = 12.18 min to MHN215. There are six isomers of MHN215 (see Table 1), which can be categorized as pinene hydroxy nitrates, endocyclic double bond oxidation limonene nitrates, and exocyclic double bond oxidation limonene nitrates. However, it remains unclear which isomers correspond to these two peaks (RT = 12.18 and 12.75 min).

3.2.2. m/z = 230 ion

Fig. 2 shows the EIC and MS^n spectrum of the parent ions at m/z = 230. One chromatographic peak appeared at 13.21 min. MS^2 spectrum obtained for the peak at RT = 13.21 min is shown in Fig. 2b, with CID energy of 25 eV. The most intense product ion occurring at m/z = 212 could be solely explained by the loss of one H_2O from the m/z = 230 parent ion. To make clear the specific structure, the product ions at m/z = 212 were further fragmented with CID energy of 35 eV (MS^3 of the m/z = 230 ion, see Fig. 2c). The product ions at m/z = 194 and 166 were most likely due to neutral losses of H_2O (18 Da) and NO_2 (46 Da) from the ions at m/z = 212, respectively. Perraud et al. (2010) confirmed that the m/z = 212 ion generated from a larger pinene nitrate with molecular mass of 229 would further fragment into a ion at m/z = 166. The neutral losses of NO_2 and H_2O are consistent with the presence of one nitrooxy group, one hydroxyl group, and one carbonyl group in PKN229 molecules. Therefore, the peak at RT = 13.21 min is assigned to PKN229. Note that there are two isomers of PKN229 (see Table 1) and either or both of them can correspond to the peak at RT = 13.21 min.

3.2.3. m/z = 248 ion

Fig. 3 shows the EIC and MS^2 spectrum of the parent ions at m/z = 248. One chromatographic peak appeared at 12.10 min. Fragmentation of the parent ions with CID energy of 25 eV generated ions at m/z = 231, 230, 213, 202, and 199. The product ions at m/z = 231, 230, 213, and 202 are explained by neutral losses of OH (17 Da), H_2O

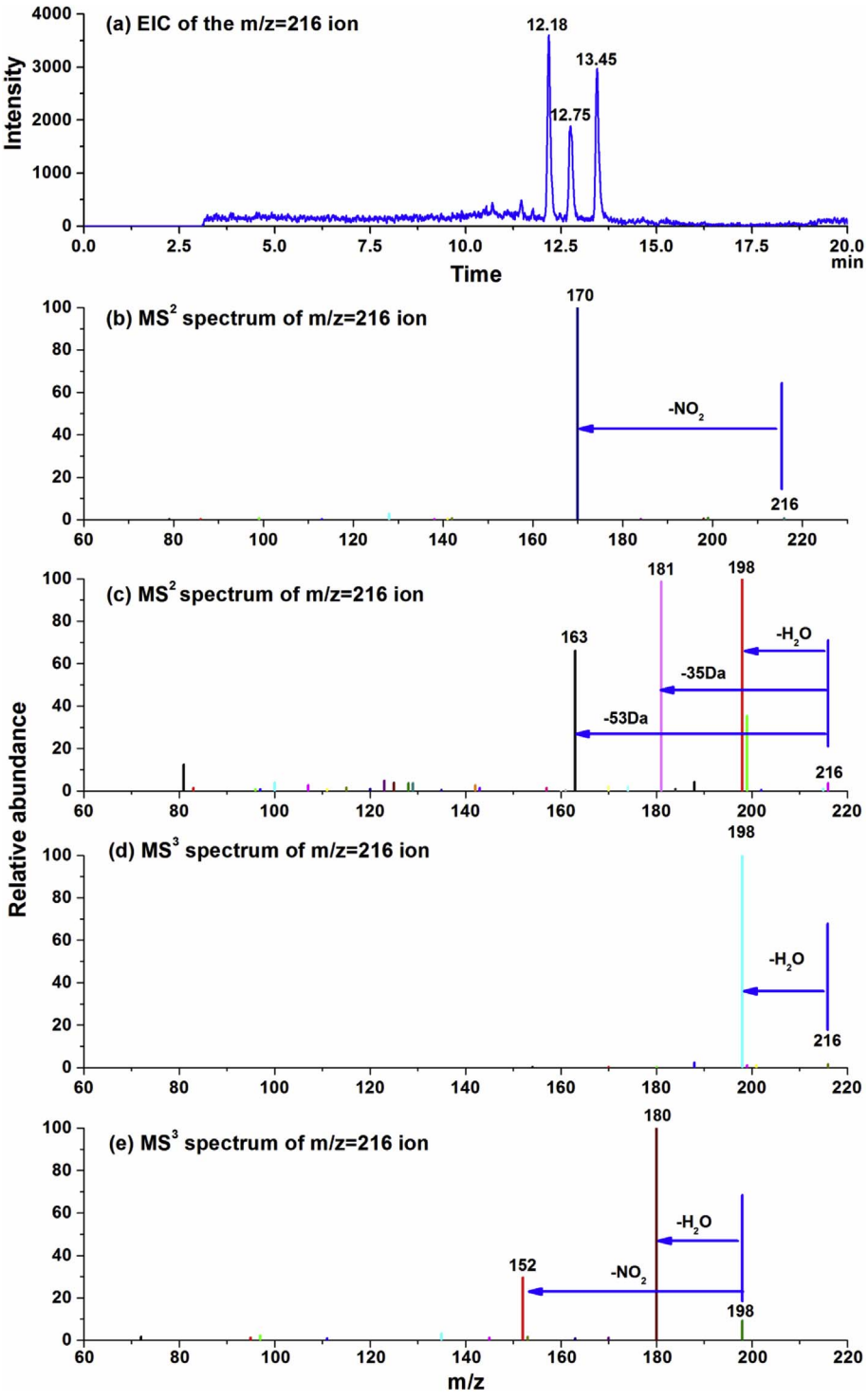

Fig. 1. EIC and MS^n spectrum of the parent ion at m/z = 216.

(18Da), OH + H_2O (35 Da), and NO_2 (46Da), respectively. They are consistent with the presence of one hydroxyl, two carbonyl, and one nitrooxy groups in LDKN247. The product ion at m/z = 199 is possibly due to the loss of OH + O_2 (49Da) or other fragments. Therefore, we assigned the peak at RT = 12.10 min to LDKN247 which has been reported in chamber simulation study by Fry et al. (2011).

3.2.4. m/z = 360 ion

The EIC and MS^2 spectrum of the parent ions at m/z = 360 are shown in Fig. 4. Only one chromatographic peak was observed at 15.75 min. The further fragmentation with CID energy of 30 eV generated two ions at m/z = 342 and 268. The product ion at m/z = 342 is explained by neutral loss of H_2O (18Da). The product ion at m/z = 268 can be explained by neutral loss of $HNO_3 + C_2H_5$ (92 Da) which is indicated by a minor mass peek at m/z = 297 (loss of HNO_3 from the parent ion). This result is consistent with the structure of OAKN359 and the peak at RT = 15.75min is therefore assigned to OAKN359.

3.2.5. m/z = 362 ion

Fig. 5 shows the EIC and MS^2 spectrum of the parent ions at m/z = 362. One chromatographic peak appeared at 13.73 min. The

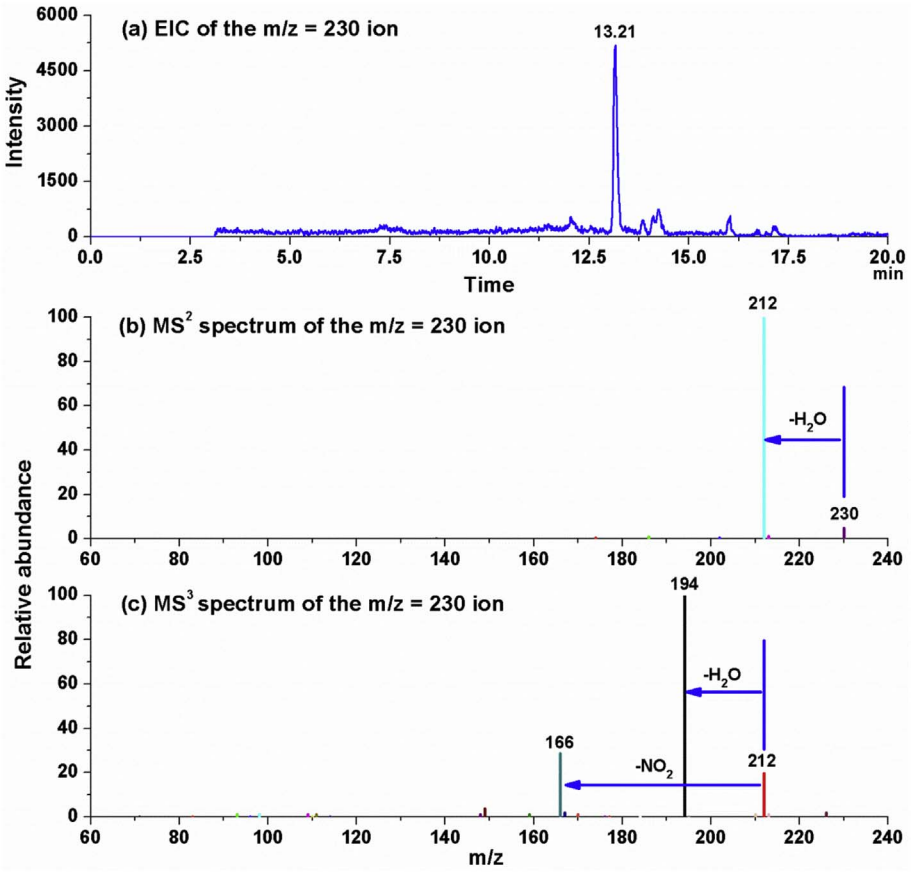

Fig. 2. EIC and MS^n spectrum of the parent ion at m/z = 230.

fragmentation of parent ions with CID energy of 25 eV generated three ions at m/z = 344, 300, and 256. The most intense mass peak at m/z = 300 corresponds to a neutral loss of 62 Da fragment from the parent ion. Two weak mass peaks at m/z = 344 and 256 correspond to neutral losses of 18 Da and 106 Da fragments from the parent ions, respectively. The 18 Da loss is naturally explained as H_2O. The 106 Da loss can be explained as $NO_3 + CO_2$. The above results are similar to the detection of oleic acid nitrate with LC/ESI-MS in chamber study by Docherty and Ziemann (2006) and are consistent with the presence of carboxyl and nirooxy groups in OAHN361. Therefore, the peak at RT = 13.73 min is assigned to OAHN361. OAKN359 and OAHN361 have been confirmed as important oxidation products of oleic acid (Docherty and Ziemann, 2006) which is the most abundant unsaturated fatty acid and widely presents in the oils or fats of living bodies (Katrib et al., 2005).

3.3. Semi-quantification of PBONs

Due to the lack of available authentic standards of the identified

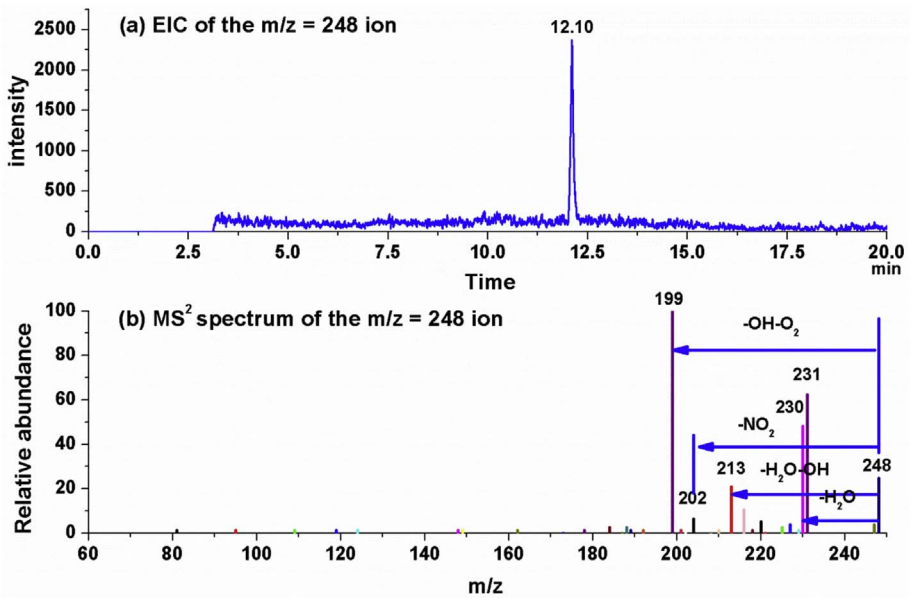

Fig. 3. EIC and MS^2 spectrum of the parent ion at m/z = 248.

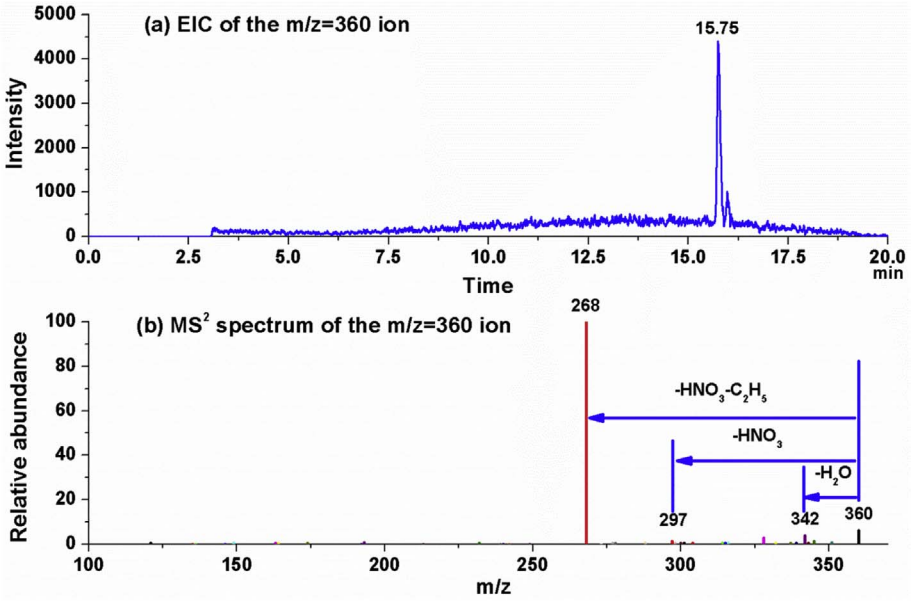

Fig. 4. EIC and MS^2 spectrum of the parent ion at m/z = 360.

PBONs, surrogate standards with similar structure or same function groups and adjacent retention time were used to obtain an approximate response of the UHPLC/ESI-MS in this study. Considering that (1R,2R,5R)-(+)-2-hydroxy-3-pinanone has the same carbon number and a similar six-membered ring with the monoterpene nitrates of MHN215, PKN229, and LDKN247, it was selected as one of the surrogate standards. Ricinoleic acid was selected as another surrogate standard due to the same carbon number and the same carboxyl, hydroxyl, and double carbon bond groups with the oleic acid nitrates of OAKN359 and OAHN361. The retention time of (1R,2R,5R)-(+)-2-hydroxy -3-pinanone (RT = 12.24 min) is quite close to monoterpene nitrates and the ricinoleic acid appears near oleic acid nitrates, suggesting the applicability of the selected surrogate standards. The response of (1R,2R,5R)-(+)-2-hydroxy-3-pinanone in the mass spectrometer was close to but lower than that of ricinoleic acid. The responses of the two surrogate standards were used to calculate the contents of three monoterpene nitrates and two oleic acid nitrates, respectively. Note that we have also tried to test carveol and several available organic nitrates including amyl nitrate, isoamyl nitrate, and isosorbide 5-mononitrate as the potential surrogate standards. However, none of them was detected by the ESI-MS under positive ion mode. The incapability of these compounds was mainly attributed to the weak polarity and the low ionization efficiency under ESI ionization condition.

Fig. 6 shows the EIC of adduct ions of (1R,2R,5R)-(+)-2-hydroxy-3-pinanone and ricinoleic acid. The pseudo molecular ion of (1R,2R,5R)-(+)-2-hydroxy-3- pinanone exhibits a mass peak at m/z = 169. As to ricinoleic acid, the two adduct ions at m/z = 299 and 281 appeared at 17.92 min, which correspond to the pseudo molecular ion $[M+H]^+$ (m/z = 299) and the followed dehydrated ion $[M + H\text{-}H_2O]^+$ (m/z = 281), respectively. The intensity of the $[M + H\text{-}H_2O]^+$ ion is well above that of the $[M+H]^+$ ion. Therefore, the standard curve of the $[M + H\text{-}H_2O]^+$ of ricinoleic acid was used to roughly quantify the contents of oleic acid nitrates. Note that there were six isomers of MHN215, but only two chromatographic peaks were observed. In addition, there were two isomers of PKN229, but only one chromatographic peak was found. It is unclear which isomer corresponds to the observed chromatographic peaks. Thus, the total signals of MHN215 and PKN229 were used to separately quantify their concentrations with

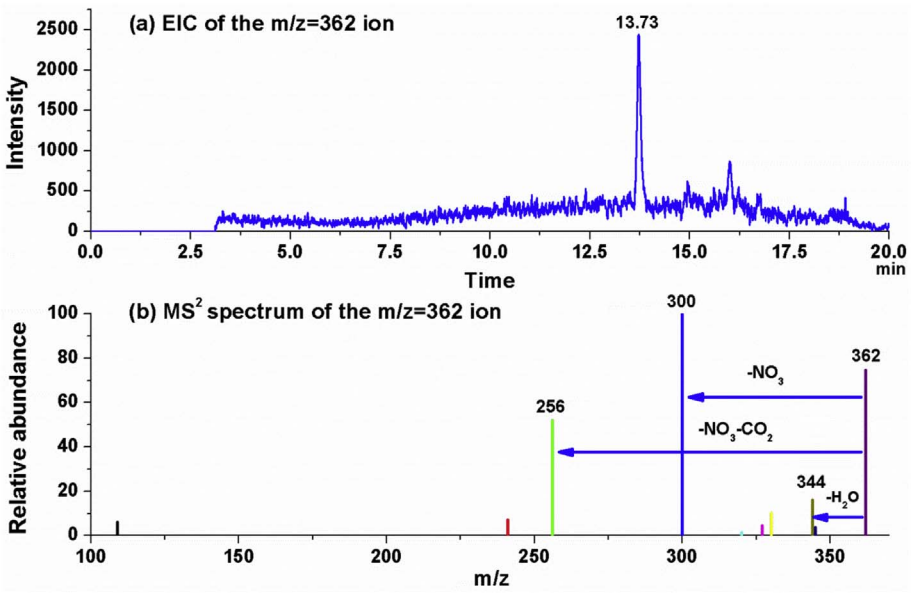

Fig. 5. EIC and MS^2 spectrum of the parent ion at m/z = 362.

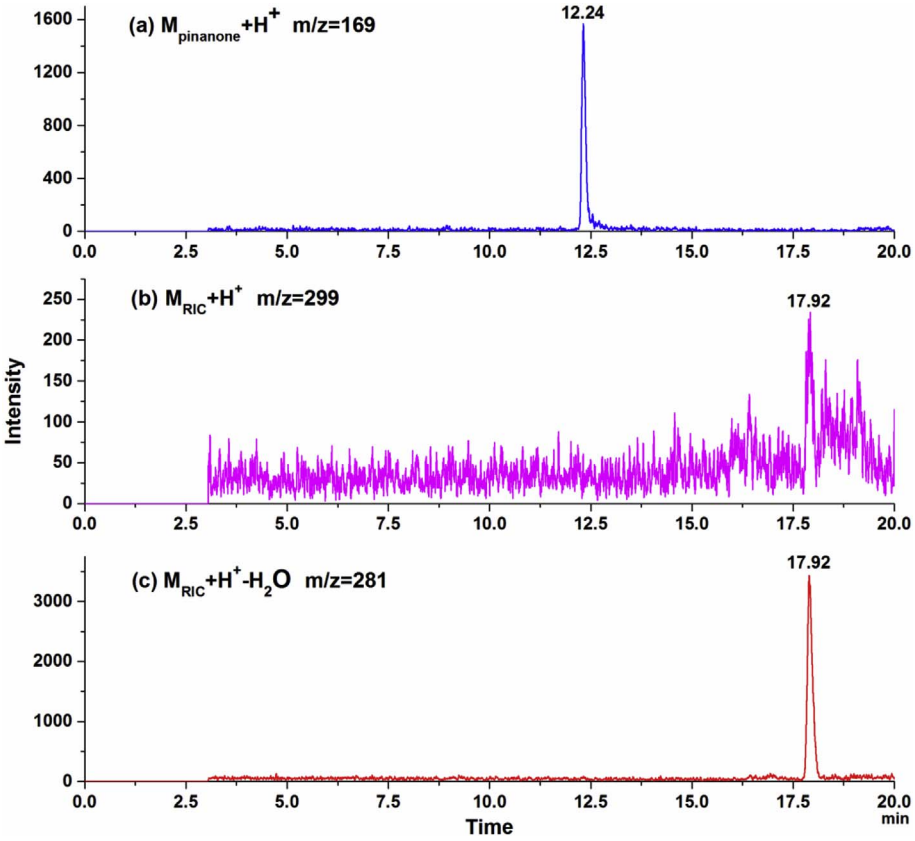

Fig. 6. EIC of adduct ions of (1R,2R,5R)-(+)-2-hydroxy-3-pinanone and ricinoleic acid.

disregarding the isomers.

3.4. Analysis of $PM_{2.5}$ sample

The contents of the identified five kinds of PBONs in $PM_{2.5}$ samples collected in urban Ji'nan in April, 2016 were calculated based on the standard curves of (1R,2R,5R)-(+)-2-hydroxy-3-pinanone and ricinoleic acid. As listed in Table 2, the average concentrations of MHN215, PKN229, LDKN247, OAKN359, and OAHN361 were 111.6 ± 23.0, 93.1 ± 49.6, 55.3 ± 7.4, 23.4 ± 14.5, 36.8 ± 18.3 ng m^{-3}, respectively. Total concentration of the five kinds of PBONs was on average 325.4 ± 116.7 ng m^{-3} (equal to 18.7 ± 6.5 ng (N) m^{-3}), contributing 1.64 ± 0.34‰ to the $PM_{2.5}$ mass concentration. The fine PBONs concentration observed in urban Ji'nan in spring was lower than the particulate organic nitrate (PON) concentration measured in Scripps Institution of Oceanography Pier of Los Angeles (coastal urban site) in spring (45 ng (N) m^{-3}) (Mylonas et al., 1991). Compared with the PON observed in a farming area nearing Roskilde in Zealand (coastal agricultural site) in spring (14 ± 5 ng (N) m^{-3}) (Nielsen et al., 1995), total aerosol phase organic nitrates concentration measured in Pike National Forest, Colorado in summer (above 20 pptv, equal to 12 ng (N) m^{-3}) (Fry et al., 2013) and particulate alkyl and multifunctional organic nitrates concentration measured in California's San Joaquin Valley (with abundant BVOCs) in summer (above 100 ng m^{-3}, equal to 7 ng (N) m^{-3}) (Rollins et al., 2012), the PBONs concentration observed in this study was slightly high. However, the mass ratio of PBONs to $PM_{2.5}$ of Ji'nan is substantially low compared to those in the above locations, which is attributed to the existence of unidentified organic nitrates, the different aerosol composition, and the high aerosol loading in urban Ji'nan during the sampling period.

Table 2
Concentrations of PBONs and the ratios to $PM_{2.5}$ in urban Ji'nan in April, 2016 (mean ± standard deviation).

PBON	Conc. ng m^{-3}	Conc. in N ng m^{-3}	PBON/$PM_{2.5}$‰
MHN215	111.6 ± 23.0	7.3 ± 1.5	0.64 ± 0.16
PKN229	93.1 ± 49.6	5.7 ± 3.0	0.52 ± 0.23
LDKN247	55.2 ± 7.4	3.1 ± 0.4	0.32 ± 0.04
OAKN359	23.4 ± 14.5	0.9 ± 0.6	0.11 ± 0.05
OAHN361	36.8 ± 18.3	1.4 ± 0.7	0.18 ± 0.06
Total	325.4 ± 116.7	18.7 ± 6.5	1.64 ± 0.34

4. Conclusions

In this study, a detection method was developed and optimized for PBONs measurement based on UHPLC/ESI-MS. Identification of PBONs was conducted on the basis of characteristic fragments of NO_2, NO_3, HNO_3, CO_2, and H_2O with the assistance of MS^n. MHN215, PKN229, LDKN247, OAKN359, and OAHN361, which were mainly generated from biogenic sources, have been identified in fine particulate matters collected in urban Ji'nan in spring. The major characteristic fragment loss of the first three monoterpene nitrates was NO_2, while the major characteristic fragment loss for the two oleic acid nitrates was NO_3. (1R,2R,5R)-(+)-2-hydroxy-3-pinanone and ricinoleic acid were used as surrogate standards to roughly quantify the contents of PBONs in particulate matters. Total concentration of the five kinds of PBONs was on average 325.4 ± 116.7 ng m^{-3}, contributing 1.64 ± 0.34‰ to the $PM_{2.5}$ mass concentration. Compared with the limited field observations of organic nitrates in urban area and forests in North America, the ratio of PBONs to $PM_{2.5}$ in urban Ji'nan was relatively low, possibly due to the unidentification of some low-polar organic nitrates (such as alkyl nitrates) or semi-volatile organic nitrates (such as isoprene nitrates) by UHPLC/ESI-MS in this study, the discrepancy in aerosol composition, and the high levels of $PM_{2.5}$ during the sampling period. Further study is required to explore the unknown organic nitrates with other advanced analytical techniques.

Acknowledgements

This work was supported by the National Key Research and Development Program of China (No. 2016YFC0200500) and the National Natural Science Foundation of China (Nos. 41775118, 91544213, 91644214).

References

Atherton, C.S., 1989. Organic nitrates in remote marine environments: evidence for long range transport. Geophys. Res. Lett. 16, 1289–1292.

Ayres, B., Allen, H., Draper, D., Brown, S., Wild, R., Jimenez, J., Day, D., Campuzano-Jost, P., Hu, W., Gouw, J.d., 2015. Organic nitrate aerosol formation via NO_3+ biogenic volatile organic compounds in the southeastern United States. Atmos. Chem. Phys. 15, 13377–13392.

Beaver, M., St Clair, J., Paulot, F., Spencer, K., Crounse, J., LaFranchi, B., Min, K., Pusede, S., Wooldridge, P., Schade, G., 2012. Importance of biogenic precursors to the budget of organic nitrates: observations of multifunctional organic nitrates by CIMS and TD-LIF during BEARPEX 2009. Atmos. Chem. Phys. 12, 5773–5785.

Bellouin, N., Rae, J., Jones, A., Johnson, C., Haywood, J., Boucher, O., 2011. Aerosol forcing in the climate model intercomparison project (CMIP5) simulations by HadGEM2-ES and the role of ammonium nitrate. J. Geophys. Res. 116, D20206.

Charlson, R.J., Schwartz, S., 1992. Climate forcing by anthropogenic aerosols. Science 255, 423.

Day, D.A., Liu, S., Russell, L.M., Ziemann, P.J., 2010. Organonitrate group concentrations in submicron particles with high nitrate and organic fractions in coastal southern California. Atmos. Environ. 44, 1970–1979.

Docherty, K.S., Ziemann, P.J., 2006. Reaction of oleic acid particles with NO_3 radicals: products, mechanism, and implications for radical-initiated organic aerosol oxidation. J. Phys. Chem. A 110, 3567–3577.

Fisher, J.A., Jacob, D.J., Travis, K.R., Kim, P.S., Marais, E.A., Chan Miller, C., Yu, K., Zhu, L., Yantosca, R.M., Sulprizio, M.P., 2016. Organic nitrate chemistry and its implications for nitrogen budgets in an isoprene-and monoterpene-rich atmosphere: constraints from aircraft (SEAC^{4}RS) and ground-based (SOAS) observations in the Southeast US. Atmos. Chem. Phys. 16, 5969–5991.

Fry, J., Draper, D., Zarzana, K., Campuzano-Jost, P., Day, D., Jimenez, J., Brown, S., Cohen, R., Kaser, L., Hansel, A., 2013. Observations of gas-and aerosol-phase organic nitrates at BEACHON-RoMBAS 2011. Atmos. Chem. Phys. 13, 8585–8605.

Fry, J., Kiendler-Scharr, A., Rollins, A., Brauers, T., Brown, S., Dorn, H.-P., Dubé, W., Fuchs, H., Mensah, A., Rohrer, F., 2011. SOA from limonene: role of NO_3 in its generation and degradation. Atmos. Chem. Phys. 11, 3879–3894.

Hallquist, M., Wängberg, I., Ljungström, E., Barnes, I., Becker, K.-H., 1999. Aerosol and product yields from NO_3 radical-initiated oxidation of selected monoterpenes. Environ. Sci. Technol. 33, 553–559.

Horowitz, L.W., Fiore, A.M., Milly, G.P., Cohen, R.C., Perring, A., Wooldridge, P.J., Hess, P.G., Emmons, L.K., Lamarque, J.F., 2007. Observational constraints on the chemistry of isoprene nitrates over the eastern United States. J. Geophys. Res. 112, D12S08.

Katrib, Y., Biskos, G., Buseck, P., Davidovits, P., Jayne, J., Mochida, M., Wise, M., Worsnop, D., Martin, S., 2005. Ozonolysis of mixed oleic-acid/stearic-acid particles: reaction kinetics and chemical morphology. J. Phys. Chem. A 109, 10910–10919.

Kwan, A., Chan, A., Ng, N., Kjærgaard, H.G., Seinfeld, J., Wennberg, P., 2012. Peroxy radical chemistry and OH radical production during the NO_3-initiated oxidation of isoprene. Atmos. Chem. Phys. 12, 7499–7515.

Mauderly, J.L., Chow, J.C., 2008. Health effects of organic aerosols. Inhal. Toxicol. 20, 257–288.

Miljevic, B., Hedayat, F., Stevanovic, S., Fairfullsmith, K.E., Bottle, S.E., Ristovski, Z.D., 2014. To sonicate or not to sonicate PM filters: reactive oxygen species generation upon ultrasonic irradiation. Aerosol Sci. Technol. 48, 1276–1284.

Mills, G.P., Hiatt-Gipson, G.D., Bew, S.P., Reeves, C.E., 2016. Measurement of isoprene nitrates by GCMS. Atmos. Meas. Tech 9, 4533–4545.

Mylonas, D.T., Allen, D.T., Ehrman, S.H., Pratsinis, S.E., 1991. The sources and size distributions of organonitrates in Los Angeles aerosol. Atmos. Environ. 25, 2855–2861.

Ng, N.L., Brown, S.S., Archibald, A.T., Atlas, E., Cohen, R.C., Crowley, J.N., Day, D.A., Donahue, N.M., Fry, J.L., Fuchs, H., 2017. Nitrate radicals and biogenic volatile organic compounds: oxidation, mechanisms, and organic aerosol. Atmos. Chem. Phys. 17, 2103.

Nielsen, T., Egeløv, A.H., Granby, K., Skov, H., 1995. Observations on particulate organic nitrates and unidentified components of NOy. Atmos. Environ. 29, 1757–1769.

Nielsen, T., Platz, J., Granby, K., Hansen, A.B., Skov, H., Egeløv, A.H., 1998. Particulate organic nitrates: sampling and night/day variation. Atmos. Environ. 32, 2601–2608.

Novakov, T., Penner, J.E., 1993. Large contribution of organic aerosols to cloud-condensation-nuclei concentrations. Nature 365, 823–826.

O'Brien, J., Shepson, P., Muthuramu, K., Hao, C., Niki, H., Hastie, D., Taylor, R., Roussel, P., 1995. Measurements of alkyl and multifunctional organic nitrates at a rural site in Ontario. J. Geophys. Res. Atmos. 100, 22795–22804.

Perraud, V., Bruns, E.A., Ezell, M.J., Johnson, S.N., Greaves, J., Finlayson-Pitts, B.J., 2010. Identification of organic nitrates in the NO_3 radical initiated oxidation of α-pinene by atmospheric pressure chemical ionization mass spectrometry. Environ. Sci. Technol. 44, 5887–5893.

Pye, H.O., Luecken, D.J., Xu, L., Boyd, C.M., Ng, N.L., Baker, K.R., Ayres, B.R., Bash, J.O., Baumann, K., Carter, W.P., 2015. Modeling the current and future roles of particulate organic nitrates in the southeastern United States. Environ. Sci. Technol. 49, 14195–14203.

Renbaum, L.H., Smith, G.D., 2009. Organic nitrate formation in the radical-initiated oxidation of model aerosol particles in the presence of NO_x. Phys. Chem. Chem. Phys. 11, 8040–8047.

Riesz, P., Berdahl, D., Christman, C.L., 1985. Free radical generation by ultrasound in aqueous and nonaqueous solutions. Environ. Health Perspect. 64, 233.

Rollins, A., Browne, E., Min, K.-E., Pusede, S., Wooldridge, P., Gentner, D., Goldstein, A., Liu, S., Day, D., Russell, L., 2012. Evidence for NO_x control over nighttime SOA formation. Science 337, 1210–1212.

Surratt, J.D., Murphy, S.M., Kroll, J.H., Ng, N.L., Hildebrandt, L., Sorooshian, A., Szmigielski, R., Vermeylen, R., Maenhaut, W., Claeys, M., 2006. Chemical composition of secondary organic aerosol formed from the photooxidation of isoprene. J. Phys. Chem. A 110, 9665–9690.

Thieser, J., Schuster, G., Schuladen, J., Phillips, G.J., Reiffs, A., Parchatka, U., Pöhler, D., Lelieveld, J., Crowley, J.N., 2016. A two-channel thermal dissociation cavity ring-down spectrometer for the detection of ambient NO_2, RO_2NO_2 and $RONO_2$. Atmos. Meas. Tech 9, 553–576.

Treves, K., Shragina, L., Rudich, Y., 2000. Henry's law constants of some β-, γ-, and δ-hydroxy alkyl nitrates of atmospheric interest. Environ. Sci. Technol. 34, 1197–1203.

Twomey, S.A., Piepgrass, M., Wolfe, T., 1984. An assessment of the impact of pollution on global cloud albedo. Tellus B 36, 356–366.

Wooldridge, P.J., Perring, A.E., Bertram, T.H., Flocke, F.M., Roberts, J.M., Singh, H.B., Huey, L.G., Thornton, J.A., Wolfe, G.M., Murphy, J.G., Fry, J.L., Rollins, A.W., LaFranchi, B.W., Cohen, R.C., 2010. Total peroxy nitrates (ΣPNs) in the atmosphere: the thermal dissociation-laser induced fluorescence (TD-LIF) technique and comparisons to speciated PAN measurements. Atmos. Meas. Tech 3, 593–607.

Xiong, F., McAvey, K., Pratt, K.A., Groff, C., Hostetler, M., Lipton, M., Starn, T., Seeley, J., Bertman, S., Teng, A., 2015. Observation of isoprene hydroxynitrates in the southeastern United States and implications for the fate of NO_x. Atmos. Chem. Phys. 15, 11257–11272.

Xu, L., Suresh, S., Guo, H., Weber, R.J., Ng, N.L., 2015. Aerosol characterization over the southeastern United States using high-resolution aerosol mass spectrometry: spatial and seasonal variation of aerosol composition and sources with a focus on organic nitrates. Atmos. Chem. Phys. 15, 7307–7336.

Zhao, X., Yinon, J., 2002. Identification of nitrate ester explosives by liquid chromatography–electrospray ionization and atmospheric pressure chemical ionization mass spectrometry. J. Chromatogr. A 977, 59–68.